BIOCHEMISTRY
including biophysical chemistry & molecular biology

Article

pubs.acs.org/biochemistry

Inverse Solvent Isotope Effects Arising from Substrate Triggering in the Factor Inhibiting Hypoxia Inducible Factor

John A. Hangasky, Evren Saban, and Michael J. Knapp*

Department of Chemistry, University of Massachusetts, Amherst, Massachusetts 01003, United States

Supporting Information

ABSTRACT: Oxygen homeostasis plays a critical role in angiogenesis, erythropoiesis, and cell metabolism. Oxygen homeostasis is set by the hypoxia inducible factor-1α (HIF-1α) pathway, which is controlled by factor inhibiting HIF-1α (FIH). FIH is a non-heme Fe(II), α-ketoglutarate (αKG)-dependent dioxygenase that inhibits HIF-1α by hydroxylating the C-terminal transactivation domain (CTAD) of HIF-1α at HIF-Asn^{803}. A tight coupling between CTAD binding and O_2 activation is essential for hypoxia sensing, making changes in the coordination geometry of Fe(II) upon CTAD encounter a crucial feature of this enzyme. Although the consensus chemical mechanism for FIH proposes that CTAD binding triggers O_2 activation by causing the Fe(II) cofactor to release an aquo ligand, experimental evidence of this has been absent. More broadly, this proposed coordination change at Fe(II) has not been observed during steady-state turnover in any αKG oxygenase to date. In this work, solvent isotope effects (SIEs) were used as a direct mechanistic probe of substrate-triggered aquo release in FIH, as inverse SIEs (SIE < 1) are signatures for pre-equilibrium aquo release from metal ions. Our mechanistic studies of FIH have revealed inverse solvent isotope effects in the steady-state rate constants at limiting concentrations of CTAD or αKG [$^{D_2O}k_{cat}/K_{M(CTAD)}$ = 0.40 ± 0.07, and $^{D_2O}k_{cat}/K_{M(\alpha KG)}$ = 0.32 ± 0.08], providing direct evidence of aquo release during steady-state turnover. Furthermore, the SIE at saturating concentrations of CTAD and αKG was inverse ($^{D_2O}k_{cat}$ = 0.51 ± 0.07), indicating that aquo release occurs after CTAD binds. The inverse kinetic SIEs observed in the steady state for FIH can be explained by a strong Fe−OH_2 bond. The stable Fe−OH_2 bond plays an important part in FIH's regulatory role over O_2 homeostasis in humans and points toward a strategy for tightly coupling O_2 activation with CTAD hydroxylation that relies on substrate triggering.

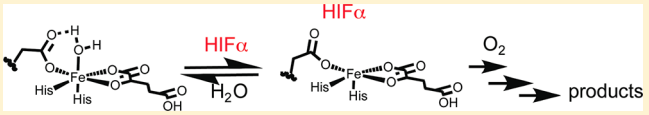

Oxygen homeostasis is essential for proper cellular function in humans and is tightly controlled by a small group of non-heme Fe(II), α-ketoglutarate (αKG)-dependent dioxygenases. Oxygen-dependent regulation of the transcriptional coactivator hypoxia inducible factor-1α (HIF-1α) maintains O_2 homeostasis as HIF-1α controls more than 100 genes, directing processes such as angiogenesis, glycolysis, and erythropoeisis.[1−3] The Fe(II)/αKG-dependent dioxygenase "factor inhibiting HIF-1α" (FIH-1 or FIH) inhibits HIF-1α in the presence of sufficient O_2 by hydroxylating the C-terminal activation domain (CTAD) of HIF-1α at HIF-Asn^{803}.[4−7] This hydroxylation prevents recruitment of the CREB binding protein, effectively downregulating HIF-1α-dependent gene expression in response to a normal or an elevated O_2 concentration.

The consensus mechanism for Fe(II)/αKG-dependent dioxygenases proposes that binding of the primary substrate triggers the Fe(II) to bind O_2, because of aquo release opening a coordination site for O_2 (Scheme 1). Substrate triggering is a central tenet of the consensus mechanism, as it can explain the relative O_2 reactivity of αKG oxygenases.[11,49] Subsequent O_2 activation allows for oxidative decarboxylation of αKG and the formation of a highly reactive ferryl intermediate. H-Atom abstraction and the ensuing $^{\bullet}$OH rebound effectively hydroxylate the primary substrate. As sensing the O_2 concentration requires that O_2 activation occur only when HIF-1α is bound, substrate triggering is the key to O_2 sensing by FIH.

Various experimental techniques have been used to test the consensus mechanism of the Fe(II)/αKG-dependent dioxygenases. Extensive spectroscopic studies of the Fe(II)/αKG-dependent dioxygenase clavaminate synthase (CAS) have provided insight into the coordination change due to aquo release induced by the primary substrate. MCD and CD studies of (Fe + αKG)CAS indicate the Fe(II) is predominantly six-coordinate. Upon addition of the primary substrate (S), the active site iron of (Fe + αKG + S)CAS adopts a five-coordinate square-pyramidal geometry[8−10] because of the release of the aquo ligand. Stopped-flow and freeze-quench techniques have been used to study the Fe(II)/αKG-dependent dioxygenase, taurine dioxygenase (TauD). Loss of the aquo ligand was observed under single-turnover conditions, and these studies identified an Fe(IV)=O intermediate as the active oxidant in TauD.[11−13] However, these studies did not address aquo release under multiple-turnover conditions, leaving open the possibility that aquo release is not a recurring step in the steady state.

Received: November 16, 2012
Revised: January 13, 2013
Published: January 25, 2013

dx.doi.org/10.1021/bi3015482 | *Biochemistry* 2013, 52, 1594−1602

Scheme 1. Consensus Chemical Mechanism for FIH

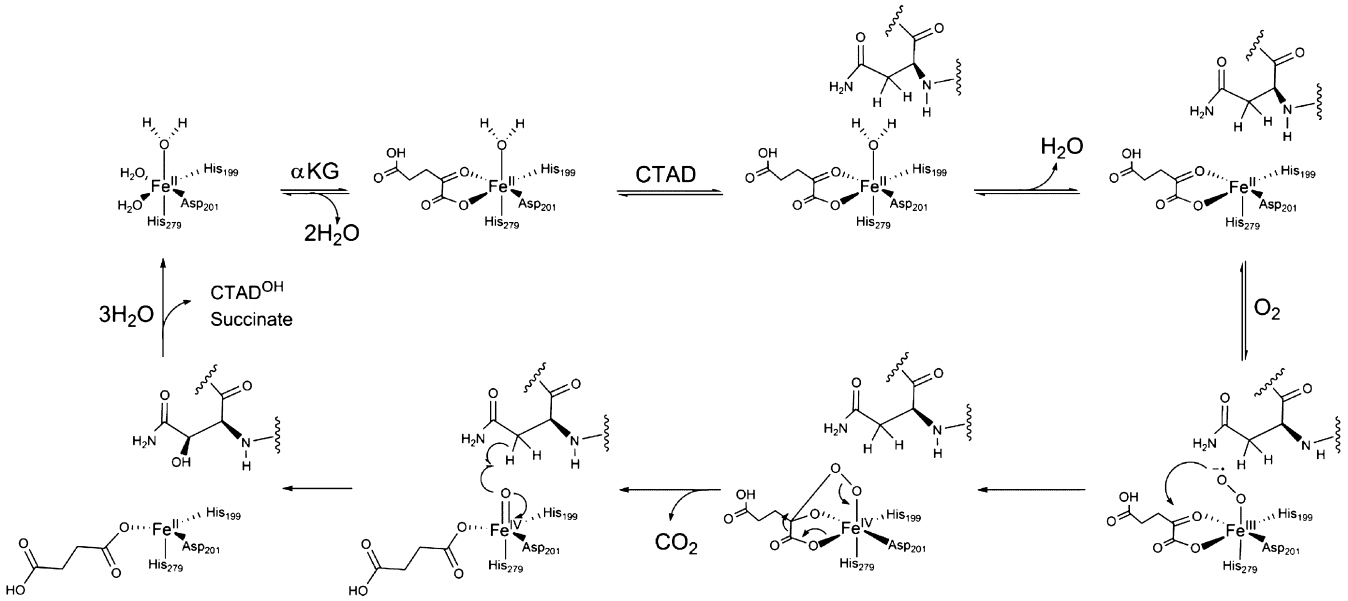

To date, neither in-depth spectroscopic studies of the coordination changes proposed upon substrate binding nor mechanistic probes for substrate triggering have been reported for FIH, making substrate triggering in this enzyme largely speculative. The X-ray crystallographic data for FIH bound to various substrates are ambiguous with respect to the coordination geometry of Fe(II), making it difficult to draw conclusions about the link between substrate binding and aquo release. Structures of (Fe + αKG)FIH are reported to contain either five-coordinate[15] or six-coordinate[16] Fe(II); however, the crystal structure of (Fe + αKG + CTAD)FIH shows a five-coordinate Fe(II),[15] suggesting that aquo release may partially occur prior to CTAD binding. EPR spectroscopy of Co(II)-substituted (Co + αKG)FIH revealed a mixture of five-coordinate and six-coordinate Co(II), further suggesting that aquo release may occur prior to CTAD binding.[17,18] Crystal structures of both (Fe + αKG + Notch)FIH and (Fe + αKG + TNKS2)FIH were refined with an axial aquo ligand present, suggesting that aquo release occurs after these substrates bind.[19,20] Direct mechanistic probes of aquo release during turnover would provide a crucial view of the mechanism of this enzyme, as well as providing insight into substrate triggering by this broad class of enzymes.

We propose that the extensive H-bonding network surrounding the active site of FIH constitutes a second coordination sphere, which transduces CTAD binding into aquo release. Steady-state kinetics of FIH point mutants indicate that removal of hydrogen bonds from several residues surrounding the Fe(II) impairs catalytic efficiency,[14] suggesting that substrate binding causes alterations of those hydrogen bonds. FIH has been shown to have a tightly coupled oxidative and reductive half-reaction, avoiding the formation of reactive oxygen species during turnover.[21] Point mutations that perturb this H-bonding network significantly decrease FIH activity and lead to uncoupled αKG consumption.[14] On the basis of FIH crystal structures and mechanistic data for point mutants, we hypothesized that aquo release occurs with every turnover during the steady state.

To test this hypothesis, we applied mechanistic probes that are sensitive to those steps preceding O_2 activation. Specifically, we focused on the steps involving αKG and CTAD binding, as these steps lead to substrate triggering: the aquo release and priming of the Fe(II) for O_2 binding and activation. Steady-state kinetic assays were performed to identify the preferred binding order for CTAD and αKG. Solvent isotope effects (SIEs) on steady-state rate constants were measured to test for the release of aquo ligands from the Fe(II) cofactor. When the rate constants are larger in D_2O-containing buffers than in H_2O-containing buffer, the kinetic SIEs are "inverse" and are diagnostic of pre-equilibrium release of aquo ligands from metal cofactors. We observed inverse SIEs on steady-state rate constants, providing direct evidence of the pre-equilibrium release of one, two, and three aquo ligands from the Fe(II) under different conditions. Our results establish two very important points. First, binding of CTAD to (Fe + αKG)FIH leads to the release of one aquo ligand, suggesting that the overall strategy for controlling hydroxylation in FIH relies on substrate-triggered changes in hydrogen bonding to release the aquo ligand. Second, the rate-limiting step in the steady state precedes or coincides with the first irreversible step; this is likely to be decarboxylation (Scheme 1), meaning that oxidized intermediates do not accumulate in FIH. Both observations point to an overall strategy for O_2 activation that relies on careful control over substrate triggering in FIH.

EXPERIMENTAL PROCEDURES

Materials. All buffers and reagents were purchased from commercial vendors and were not further purified, with the exception of the CTAD peptide. The CTAD peptide corresponding to the C-terminal activation domain of human HIF-1α (HIF-1$\alpha^{788-826}$) contained a Cys^{800} → Ala point mutation[21] (DESGLPQLTSYDAEVNAPIQGSRNLLQGEEL-LRALDQVN). The CTAD peptide was purchased as a desalted peptide from EZBiolab (Carmel, IN) with free N- and C-termini. Reverse phase high-performance liquid chromatography (RP-HPLC) utilizing a gradient from 30% acetonitrile and 0.1% trifluoroacetic acid (TFA) to 95% acetonitrile and 0.1% TFA was used to obtain >95% pure CTAD.

Protein Expression and Purification. FIH was overexpressed in *Escherichia coli* with an N-terminal His_6 tag and

dx.doi.org/10.1021/bi3015482 | *Biochemistry* 2013, 52, 1594−1602

purified as previously described.[18] Briefly, His_6-FIH was separated from cell lysate via Ni-NTA column chromatography and the affinity tag was then cleaved with thrombin. Three additional residues from the fusion protein (NH_2-GlySerHis-) remained on the N-terminus following thrombin cleavage. Cleaved FIH was collected as flow-through from a Ni-NTA column and then incubated with EDTA to removed metal. Dimeric FIH was obtained via size-exclusion chromatography using Sephadex G-75 resin and 50 mM NaCl and 50 mM Tris (pH 8.00) as the running buffer. Purified FIH was buffer exchanged into 50 mM HEPES (pH 7.00). The molecular mass was confirmed by QSTAR TOF-MS (expected, 40.566 kDa; observed, 40.574 kDa), while the purity (>95%) was assessed by sodium dodecyl sulfate−polyacrylamide gel electrophoresis.

Steady-State Kinetic Assays. All assays were performed at 37.0 °C with saturating concentrations of $FeSO_4$ (50 μM) and ascorbate (2 mM) and an ambient O_2 concentration. Assays in which CTAD was the varied substrate (15−250 μM) utilized a saturating level of αKG (500 μM) unless specified otherwise. Assays with αKG as the varied substrate (5−200 μM) utilized a fixed CTAD concentration of either 39 μM [$\sim {}^1/_2 K_{M(CTAD)}$] or 306 μM [$\sim 4K_{M(CTAD)}$]. Assay reagents were mixed and incubated for 2 min at 37.0 °C in microcentrigue tubes. Then the reaction was initiated via the addition of enzyme ($[E]_T$ = 0.5 μM). Reaction aliquots (5 μL) were quenched with 75% acetonitrile and 0.2% TFA (20 μL) saturated with 3,5-dimethoxy-4-hydroxycinnamic acid and analyzed for peptide hydroxylation using a Bruker Daltonics Omniflex MALDI-TOF-MS instrument. The mole fraction of product, $\chi_{CTAD\text{-}OH}$, was determined by the relative intensities of hydroxylated CTAD ($CTAD^{OH}$, m/z 4271) and unhydroxylated CTAD (m/z 4255). Initial rates were determined from five to seven quenched time points. The steady-state rate constants, k_{cat} and k_{cat}/K_M, were obtained by nonlinear least-squares fitting of initial rate data (0 to ∼15% fractional conversion) to the Michaelis−Menten equation.

Viscosity Assays. Steady-state assays were performed in 50 mM HEPES (pH 7.00), using sucrose as the viscosogen to test for the rate limitation of diffusional steps. Initial rates were measured as described above, using buffers containing 10% (η_{rel} = 1.3), 18% (η_{rel} = 1.8), and 25% (η_{rel} = 2.8) sucrose solutions (w/w).[22]

Solvent Isotope Assays. Deuterium oxide (D, 99.9%) was purchased from Cambridge Isotope Laboratories (Andover, MA) and used as received. The pD was determined by presoaking the pH meter in D_2O for 10 min and then adding 0.4 to the meter reading of the D_2O solution of interest (pD = pH_{read} + 0.4).[23] Steady-state assays were performed as described above. All reagent stocks used in the steady-state assays in D_2O were prepared using D_2O. Working FIH stock solutions were made by diluting high-concentration stocks from H_2O into D_2O containing 50 mM HEPES (pD 7.00). Assays were performed in 50 mM HEPES (pD 7.00) with a final D_2O percentage of 97%. SIEs were calculated from the ratio of rate constants observed in buffers containing H_2O or D_2O; e.g., ${}^{D_2O}k_{cat} = k_{cat(H_2O)}/k_{cat(D_2O)}$.

Coupling Ratio. The extent of coupling between FIH's two half-reactions in D_2O was determined from monitoring the succinate and $CTAD^{OH}$ concentrations throughout a reaction. Reactions of αKG (500 μM), $FeSO_4$ (50 μM), CTAD (200 μM), and FIH (5 μM) were performed in 50 mM Tris (pD 7.00) and analyzed using procedures similar to those previously reported.[14,24] A Hamilton PRP-X300 anion exclusion column was used to separate the succinate produced from the quenched reactions. UV detection at 210 nm was used to determine the succinate concentration. Using aliquots from the same quenched assay, a Bruker Daltonics Omniflex MALDI-TOF-MS instrument was used to determine the $CTAD^{OH}$ concentration. The coupling ratio (C) was determined by fitting the succinate concentration as a linear function of $CTAD^{OH}$ concentration for multiple quench points, where C = [succinate]/[$CTAD^{OH}$].

RESULTS

Solvent Isotope Effects. Solvent isotope effects (SIEs) were measured to test for aquo release from the Fe(II) as part of substrate triggering during turnover in FIH. By varying the degree of saturation with respect to αKG and CTAD, we accessed the SIE on kinetic constants reporting on different microscopic steps. SIEs arising from the pre-equilibirum release of one, two, and three aquo ligands were predicted from the consensus mechanism, depending on the assay conditions (Scheme 1). As the limiting SIEs are multiples of the proton fractionation factor (Φ) for the O−L bond (L = H or D),[25] they are quite distinct for the number of aquo ligands released.

The fractionation factor for L_2O (where L = H or D) is inverse when water is bonded to another Lewis acid, leading to a tendency for D_2O to accumulate in bulk solvent. For example, $\Phi_{O\text{-}L}$ = 0.69 for L_3O^+ [26−28] because of zero-point energy differences. The fractionation factor, $\Phi_{O\text{-}L}$, for aquo release from Co(II) in two carbonic anhydrase isozymes has been found to be between 0.72 and 0.90,[25,29] agreeing closely with the fractionation factor for $Co(H_2O)_6^{2+}$ in solution ($\Phi_{O\text{-}L}$ = 0.73).[30] As the fractionation factor for the Fe^{2+}−OH_2 bond in FIH is unknown, we estimate Φ = 0.70 as is commonly done for fractionation of water from other M−OH_2 ⇌ M + OH_2 equilibria.[30] As Φ is reported on a per-bond basis and is multiplicative, ${}^{D_2O}K_{eq}$ values for the release of aquo ligands are diagnostic of the numbers of H_2O molecules released from Fe: one (${}^{D_2O}K_{eq} = \Phi^2 = 0.49$), two (${}^{D_2O}K_{eq} = \Phi^4 = 0.24$), and three (${}^{D_2O}K_{eq} = \Phi^6 = 0.12$).

The equilibrium fractionation factors will lead to inverse kinetic SIEs on different kinetic constants provided that the aquo release is in a pre-equilibrium prior to a subsequent rate-limiting step. As shown in the Appendix, k_{cat} and $k_{cat}/K_{M(CTAD)}$ can report on one aquo release, leading to the prediction that the limiting values for ${}^{D_2O}k_{cat} \sim {}^{D_2O}[k_{cat}/K_{M(CTAD)}] = 0.49$. In contrast, the limiting values for ${}^{D_2O}[k_{cat}/K_{M(\alpha KG)}]$ will report on the release of two or three aquo ligands depending on the degree to which FIH is saturated with CTAD. It is important to note that our assays used an ambient O_2 concentration (220 μM), which is approximately $2K_{M(O_2)}$,[31] making our kinetic constants apparent.

The rate constants obtained at a saturating αKG concentration, an ambient O_2 concentration, and varied CTAD concentrations are k_{cat} and $k_{cat}/K_{M(CTAD)}$. Under these conditions, k_{cat} reports on all steps from CTAD binding to product release and is predicted to involve the release of one aquo ligand (Scheme 1). The initial rate assays in D_2O exhibited increased rates when compared to similar assays in H_2O, indicating an inverse SIE on both k_{cat} and $k_{cat}/K_{M(CTAD)}$. We observed a ${}^{D_2O}k_{cat}$ of 0.51 ± 0.07, in good agreement with the limiting SIE (0.49) for the pre-equilibrium release of one aquo ligand (Figure 1). Similarly, we observed a ${}^{D_2O}[k_{cat}/$

dx.doi.org/10.1021/bi3015482 | Biochemistry 2013, 52, 1594−1602

$K_{M(CTAD)}$] of 0.40 ± 0.07, which is also in good agreement with one aquo release prior to a rate-limiting step.

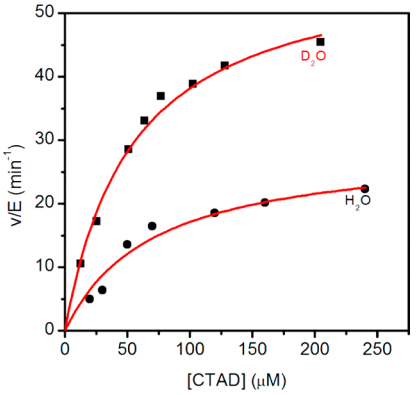

Figure 1. Steady-state kinetics of FIH in H_2O (●) and 97% D_2O (■) buffers. FIH (0.5 μM), ascorbate (2 mM), αKG (500 μM), $FeSO_4$ (50 μM), and CTAD (0–250 μM) were in 50 mM HEPES (pL 7.00).

Because of the sequential ordered mechanism (see below), the apparent $k_{cat}/K_{M(\alpha KG)}$ encompasses distinct steps depending on the fixed concentration of CTAD. Because $k_{cat}/K_{M(\alpha KG)}$ reports on steps from the encounter with αKG through the first irreversible step, high or low fixed concentrations of CTAD were used to isolate different microscopic steps. CTAD binding is kinetically irreversible at high CTAD concentrations, meaning that $k_{cat}/K_{M(\alpha KG)High[CTAD]}$ reports on only those steps between αKG encounter and CTAD binding, encompassing the release of two aquo ligands. The observed SIE of 0.32 ± 0.08 on $k_{cat}/K_{M(\alpha KG)High[CTAD]}$ was in reasonable agreement with the limiting value (0.24) expected for the release of two aquo ligands. In contrast, CTAD binding is kinetically reversible at subsaturating CTAD concentrations, making a subsequent step (thought to be O_2 activation) the first irreversible step. Thus, $k_{cat}/K_{M(\alpha KG)Low[CTAD]}$ reports on all steps between αKG binding and O_2 activation, which encompasses the release of three aquo ligands in the consensus mechanism. The observed SIE of 0.11 ± 0.03 for $k_{cat}/K_{M(\alpha KG)Low[CTAD]}$ agreed closely with the limiting value (0.12) expected for the release of three aquo ligands prior to a rate-limiting step (Figure 2).

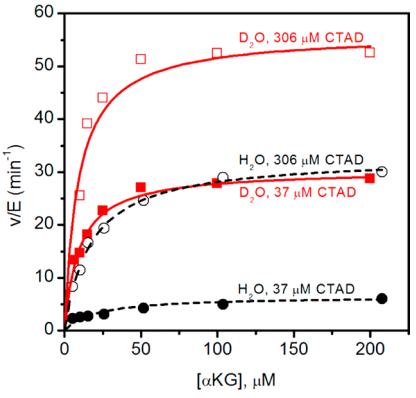

Figure 2. Steady-state kinetics of FIH for αKG at 37 μM CTAD and 306 μM CTAD, in H_2O (● and ■) and D_2O (○ and □) at 37.0 °C. FIH (0.5 μM), ascorbate (2 mM), αKG (0–210 μM), $FeSO_4$ (50 μM), and CTAD (37 and 306 μM) were in 50 mM HEPES (pL 7.00).

Validation of Observed SIEs. A series of control experiments were completed to ensure that the SIEs arose from aquo release. Control assays showed the steady-state rate constants, k_{cat} and $k_{cat}/K_{M(CTAD)}$, were pH-independent between pH 6.50 and 8.00 at a fixed ionic strength (I = 120 mM). Furthermore, steady-state assays at pH 7.00 showed that k_{cat} and $k_{cat}/K_{M(CTAD)}$ were independent of ionic strength (Figure S1 of the Supporting Information). Viscosity experiments were completed as a control for the increased relative viscosity of D_2O, as solvent viscosity can affect the rate of diffusional steps, or of conformational changes. The binding order of αKG and CTAD was also investigated to define the chemical steps reported on by $k_{cat}/K_{M(CTAD)}$ and $k_{cat}/K_{M(\alpha KG)}$, as these rate constants proved different microscopic steps within the chemical mechanism reporting the release of up to three aquo ligands.

FIH's activity increased approximately 2-fold in D_2O, prompting us to check the coupling between the oxidative and reductive half-reactions in D_2O. As the oxidative half reaction produces succinate, and the reductive half-reaction produces $CTAD^{OH}$, the [succinate]/[$CTAD^{OH}$] ratio is equal to the coupling between these half-reactions (C = [succinate]/[$CTAD^{OH}$]). Previously, we showed tight coupling between succinate production and CTAD hydroxylation in H_2O.[14] Here we observed that FIH's two half-reactions remained tightly coupled in D_2O, with C equal to unity within experimental uncertainty (C = 1.1 ± 0.1) (Table 1).

Table 1. Coupling of Succinate and $CTAD^{OH}$ Concentrations for FIH in 50 mM Tris (pL 7.00) at 37.0 °C

	C^a
D_2O	1.1 ± 0.1[b]
H_2O	0.98 ± 0.03[c]

[a] C = (moles of succinate)/(moles of $CTAD^{OH}$). [b] Reaction mixtures contained αKG (500 μM), $FeSO_4$ (50 μM), CTAD (200 μM), and FIH (5 μM) in 50 mM Tris (pD 7.00). [c] From ref 14.

Diffusional Steps Are Not Rate-Limiting. Steady-state rate constants were measured as a function of relative viscosity to test for diffusional steps that might contribute to the observed rate constants and SIEs, as the viscosity of D_2O is greater than that of H_2O. Initial rate data were collected in 50 mM HEPES (pH 7.00) with sucrose as the viscosogen and fit to the Michaelis–Menten equation. Analysis of k_{cat}, $k_{cat}/K_{M(CTAD)}$, and $k_{cat}/K_{M(\alpha KG)}$ as a function of relative viscosity indicated that each of the steady-state rate constants was independent of solvent viscosity (Figure S2 of the Supporting Information).

The normalized regression plot showed that relative viscosity had no effect on any rate constant. Thus, neither diffusional encounter, relevant for k_{cat}/K_M, nor product release, relevant for k_{cat}, is rate-limiting. If diffusional encounter were rate-limiting, k_{cat}/K_M would decrease as the relative solvent viscosity increases.[32,33] Furthermore, the lack of a viscosity effect indicates FIH does not undergo a viscosity-sensitive conformational change, which has been shown to obscure SIEs for some enzymes.[34,35]

Sequential Order: αKG Binds before CTAD. The consensus mechanism for αKG oxygenases is a sequential ordered model that, when applied to FIH, predicts αKG binds prior to CTAD. Although steady-state analyses of several other αKG-dependent oxygenases have been shown to follow this

dx.doi.org/10.1021/bi3015482 | Biochemistry 2013, 52, 1594–1602

binding order,[36−38] we tested this sequential binding model for FIH because of the interesting SIEs that we observed at varied CTAD concentrations. As the binding order of αKG and CTAD affects the microscopic steps defined by the steady-state kinetic parameters, this is critical to our interpretations of the SIEs.

Four different fixed CTAD concentrations, ranging from $^{1}/_{2}K_{M(CTAD)}$ to $4K_{M(CTAD)}$, were chosen for steady-state kinetic assays in which the αKG concentration was the varied substrate. In close agreement with previously reported values,[14,31] the $K_{M(\alpha KG)}$ remained constant at 20 ± 2 μM for all CTAD concentrations. The regression plot of $k_{cat}/K_{M(\alpha KG)}$ as a function of CTAD concentration passed through the origin, as expected for ordered sequential binding of αKG prior to CTAD (Figure 3).[39]

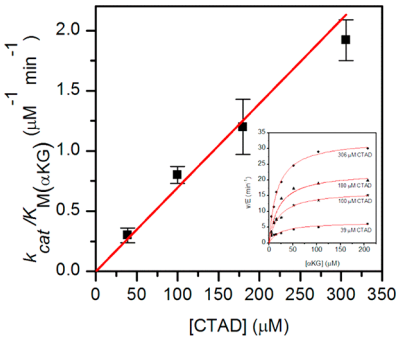

Figure 3. Regression plot showing $k_{cat}/K_{M(\alpha KG)}$ as a function of CTAD concentration. The inset shows the steady-state kinetics of FIH with αKG as the varied substrate, at different fixed CTAD concentrations at 37.0 °C. FIH (0.5 μM), ascorbate (2 mM), αKG (0−210 μM), $FeSO_4$ (50 μM), and CTAD (39−306 μM) were in 50 mM HEPES (pH 7.00).

DISCUSSION

Sensing of O_2 by FIH is critical to cellular growth and development, yielding close consonance between O_2 concentration and the FIH-catalyzed hydroxylation of CTAD central to O_2 homeostasis. An additional benefit is that controlled O_2 activation by FIH would prevent ROS production,[21] preventing anomalous oxidations. Although it has been shown that decarboxylation of αKG and hydroxylation of CTAD by FIH are tightly coupled,[14] the mechanistic strategy used by FIH to ensure that O_2 activation leads to CTAD hydroxylation with high fidelity remains unclear. Our overall hypothesis is the hydrogen bonding from the second coordination sphere ensures that the Fe(II) in (Fe + αKG)FIH remains six-coordinate, and that CTAD binding alters these hydrogen bonds leading to O_2 activation, the substrate triggering model. CTAD binding could trigger FIH by affecting any of the microscopic steps in the overall chemical mechanism, so long as the rate of O_2 activation were increased upon CTAD binding. Our observation of inverse SIEs on $k_{cat}/K_{M(CTAD)}$ and $k_{cat}/K_{M(\alpha KG)}$ indicates that the rate-limiting step in the steady state follows aquo release and is either coincident with or precedes decarboxylation (Scheme 1). This points to a strategy for tightly coupling O_2 activation with CTAD hydroxylation that relies on substrate triggering.

O_2 Activation Is Rate-Limiting in FIH. Inverse kinetic SIEs (SIE < 1) are diagnostic of aquo release from metal ions, as the vast majority of SIEs are normal (SIE > 1).[29] Two other causes of inverse kinetic SIEs, the involvement of a CysS nucleophile in catalysis and a conformational change, were ruled out for FIH. In the former case, there are no active site CysSH residues; in the latter case, we verified that viscosity did not affect the rate of turnover.

Inverse kinetic SIEs have been reported for several metalloenzymes, including a number of hydrolases, carbonic anhydrase, and a point mutant of SLO.[29,40−43] In each case, the inverse kinetic SIEs indicated that aquo release was a pre-equilibrium step prior to a subsequent rate-limiting step. Our observation of inverse kinetic SIEs corresponding to multiple aquo release steps is the first such report, to the best of our knowledge. The inverse SIEs arise from an unfavorable equilibrium for aquo release, combined with a slow O_2 activation step.

The consensus mechanism predicts that both k_{cat} and $k_{cat}/K_{M(CTAD)}$ encompass one aquo release for a limiting predicted SIE of 0.49. The experimentally observed kinetic SIEs correlate nicely with the theoretical value expected for the equilibrium release of one aquo ligand, as $^{D_2O}k_{cat}$ = 0.51 ± 0.07 and $^{D_2O}k_{cat}/K_{M(CTAD)}$ = 0.40 ± 0.07 (Table 2) A kinetic model with separate microscopic steps for αKG, CTAD, and O_2 binding, as well as the final aquo release, was constructed from the consensus chemical mechanism and used to analyze the observed SIEs (Scheme 2). As k_{cat} encompasses all steps with the exception of the diffusional encounter with substrates, a separate, reversible microscopic step for aquo release was needed, as a $^{D_2O}k_{cat}$ of <1 indicated that aquo release must be separate from CTAD encounter.

The similarity in the SIEs for k_{cat} and $k_{cat}/K_{M(CTAD)}$ strongly suggests that the overall rate-limiting step in FIH turnover is common to both rate constants. As $k_{cat}/K_{M(CTAD)}$ encompasses steps between CTAD encounter and the first irreversible step, the common step has to be the O_2 activation step (Scheme1). This step is typically viewed as the initial attack on the 2-oxo group of αKG that leads to oxidative decarboxylation. This is noteworthy as this predicts that the ferryl intermediate will not accumulate in FIH during turnover, in contrast to TauD.[12] Slow O_2- activation can account for the tight coupling between

Table 2. Solvent Isotope Effects for FIH in 50 mM HEPES (pL 7.00) at 37.0 °C

	H_2O	D_2O	experimental SIE	theoretical SIE	no. of aquo ligands
k_{cat} (min^{-1})[a]	30 ± 2.5	59 ± 2.0	0.51 ± 0.07	0.49	1
$k_{cat}/K_{M(CTAD)}$ (μM^{-1} min^{-1})[a]	0.43 ± 0.10	1.09 ± 0.11	0.40 ± 0.07	0.49	1
$k_{cat}/K_{M(\alpha KG)High[CTAD]}$ (μM^{-1} min^{-1})[b]	1.94 ± 0.13	6.05 ± 1.37	0.32 ± 0.08	0.24	2
$k_{cat}/K_{M(\alpha KG)Low[CTAD]}$ (μM^{-1} min^{-1})[c]	0.29 ± 0.07	2.60 ± 0.34	0.11 ± 0.03	0.12	3

[a]CTAD as the varied substrate; FIH (0.5 μM), ascorbate (2 mM), αKG (500 μM), $FeSO_4$ (50 μM), and CTAD (0−250 μM). [b]αKG as the varied substrate; FIH (0.5 μM), ascorbate (2 mM), αKG (5−200 μM), $FeSO_4$ (50 μM), and CTAD (306 μM). [c]αKG as the varied substrate; FIH (0.5 μM), ascorbate (2 mM), αKG (5−200 μM), $FeSO_4$ (50 μM), and CTAD (37 μM).

dx.doi.org/10.1021/bi3015482 | Biochemistry 2013, 52, 1594−1602

Scheme 2. Proposed Kinetic Mechanism for FIH (S = CTAD)

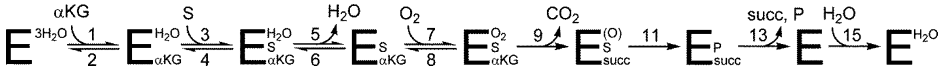

decarboxylation and hydroxylation seen for FIH[14] as hydroxylation must be very fast relative to the decarboxylation step. Thus, we conclude that FIH likely adopts a strategy to ensure tight coupling between O_2 binding and activation in which O_2 activation is rate-limiting.

We analyzed the observed kinetic SIEs using language predominately developed by Northrop and Cleland,[44,45] in which observed kinetic SIEs are a function of "commitments to catalysis" and the equilibrium and kinetic isotope effects ($^{D_2O}K_{eq}$ and $^{D_2O}K_5$, respectively) on the aquo release step (k_5). The commitments to catalysis, C_f and C_r, are ratios of microscopic rate constants that describe the tendency of an enzyme to go forward and backward, respectively, through the isotopically sensitive step. Full expressions are provided in the Appendix. In the case of $^{D_2O}k_{cat}/K_{M(CTAD)}$, this expression takes the form of eq 1. The primary virtue of such a presentation is that it permits us to focus on specific segments of the kinetic mechanism. As equilibrium isotope effects reflect fractionation factors, the equilibrium SIE on aquo release is predicted to be ~0.5 ($^{D_2O}K_5 = 0.49$).

$$^{D_2O}\left[\frac{k_{cat}}{K_{M(CTAD)}}\right] = \frac{^{D_2O}k_5 + C_f + C_r\,^{D_2O}K_5}{1 + C_f + C_r} \quad (1)$$

It is clear that the only way for $^{D_2O}k_{cat}/K_{M(CTAD)}$ to equal $^{D_2O}K_{eq}$ is for the reverse commitment to be very large ($C_r \gg C_f$). Reverse commitment (C_r) is the kinetic competition between H_2O and O_2 for the triggered form of enzyme; when C_r is large, it means that H_2O is the preferred ligand (Appendix, eq A10). Furthermore, the C_f/C_r ratio is, to a first approximation, the equilibrium for aquo release; when $C_f/C_r \ll 1$, it means that K_5 is much less than one and that the position of this equilibrium favors the aquo-on state. Similar analysis of the commitment factors for $^{D_2O}k_{cat}$ further supports the conclusion that aquo release is disfavored thermodynamically, despite a slightly different SIE expression and forward commitment on k_{cat} (C_{vf}) (Appendix).

Substrate Triggering Is Faster Than O_2 Activation. Steps involved in substrate triggering were accessed by measuring the kinetic SIE with a subsaturating αKG concentration. As $k_{cat}/K_{M(\alpha KG)}$ includes steps between diffusional encounter of αKG with FIH and the subsequent irreversible step, CTAD binding and substrate triggering may be observable on this kinetic constant. At high CTAD concentrations, only the two aquo ligands released upon αKG binding may be observed, as a saturating level of FIH with CTAD makes CTAD binding kinetically irreversible for $k_{cat}/K_{M(\alpha KG)High[CTAD]}$. In contrast, a subsaturating CTAD concentration makes it possible to access release of all three aquo ligands on $k_{cat}/K_{M(\alpha KG)Low[CTAD]}$, provided that a later step is rate-limiting.

The observed SIE for $k_{cat}/K_{M(\alpha KG)High[CTAD]}$ (SIE = 0.32 ± 0.08) correlates well with the pre-equilibrium release of two aquo ligands (Table 2), as expected for kinetically irreversible CTAD binding. The key observation supporting rapid substrate triggering was the SIE on $k_{cat}/K_{M(\alpha KG)Low[CTAD]}$ (SIE = 0.11 ± 0.03), as this indicated the pre-equilibrium release of all three aquo ligands prior to a subsequent rate-limiting step. This establishes that steps associated with CTAD binding and substrate triggering are not slow under these conditions and further points to O_2 activation as the rate-limiting step.

Hydrogen Bonding from the Second Coordination Sphere. Turnover in FIH and other αKG oxygenases depends on substrate triggering, minimally the release of the aquo ligand from the (Fe + αKG + Substr) enzyme form, prior to O_2 binding. What is striking about the kinetics of FIH are the inverse kinetic SIEs, implicating slow O_2 activation in this enzyme. In the case of FIH, substrate triggering leads to rate-limiting O_2 activation, meaning that the intermediate that is expected to accumulate in the steady state is a relatively innocuous Fe^{2+} center. In contrast, TauD exhibits SIEs of unity,[46] and the partially rate-limiting steps include product release and H-atom transfer by the $[Fe^{IV}O]^{2+}$ intermediate.[11] For TauD, substrate triggering leads to rapid O_2 activation, and the partial accumulation of a powerful oxidant, $[Fe^{IV}O]^{2+}$.[12] It is as if TauD were built for speed but FIH built for fidelity. As the ligands to the Fe(II) are identical in these two enzymes, the reasons for such disparate strategies for the oxidation reaction must lie beyond the primary coordination sphere.

We attribute the difference in oxidation strategies between these enzymes to their second coordination spheres. The most striking difference between their second coordination spheres is in the hydrogen bonding between the facial triad Asp^{201} ligand and the axial aquo ligand. In FIH, the remote O atom of Asp^{201} forms a 2.8 Å hydrogen bond to the bound aquo ligand in (Fe + αKG)FIH (Figure 4); once CTAD binds, two new hydrogen

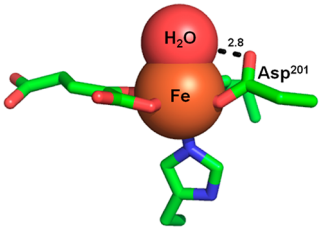

Figure 4. FIH active site with the 2.8 Å Asp^{201}–aquo hydrogen bond (Protein Data Bank entry 3P3P).

bonds form to the Asp^{201}, which appear to serve to partially stimulate aquo release.[16,17] The extensive hydrogen bonding to this aquo ligand likely serves to stabilize the Fe–OH_2 bond, which would explain the large reverse commitments to catalysis (C_r) and the inverse SIEs. Such high affinity for the aquo ligand could serve to throttle back the oxidation reaction such that O_2 activation occurs only when CTAD is present. We note a certain similarity to the hydrogen bonding network found in PHD2, which leads to an inverse $^{D_2O}k_{cat}$[47] and the absence of any accumulating intermediates in pre-steady-state experiments.[24]

TauD is a significant contrast to FIH, structurally and kinetically. The facial triad Asp of TauD is rotated away from the aquo ligand and cannot form a hydrogen bond to the bound aquo ligand. This leads to a weak Fe^{2+}–OH_2 bond strength,[48] and TauD readily activates O_2 in the absence of the substrate taurine.[49,50] The second coordination sphere of TauD

dx.doi.org/10.1021/bi3015482 | Biochemistry 2013, 52, 1594–1602

favors aquo release, which can lead to rapid O_2 activation; unfortunately, this leads to a decrease in fidelity.

CONCLUSION

Inverse kinetic SIEs on k_{cat}/K_M and k_{cat} limit the possible rate-limiting step for FIH to a step between aquo release and decarboxylation (Scheme 1). This points to a step very early in the catalytic cycle, such as O_2 activation, as the likely rate-limiting step. Such a strategy would aid in FIH's regulatory role over O_2 homeostasis in humans, as it would lead to direct transduction of intracellular O_2 levels into a readable signal, hydroxylated HIF-Asn^{803}. This tight control over O_2 activation strongly suggests that oxidized intermediates will not accumulate in FIH under normal turnover conditions and may reflect the demands of a regulatory function in O_2 sensing by tightly correlating O_2 activation with substrate hydroxylation.

APPENDIX

As there are multiple isotope-sensitive steps for the kinetic mechanism of FIH (Scheme 2), algebraic expressions for each kinetic parameter were derived using the net rate method of Tian.[51] The expression for $^{D_2O}k_{cat}$ takes the form

$$^{D_2O}(k_{cat}) = \frac{^{D_2O}k_5 + {}^{D_2O}k_{15}C_{Vf} + C_r{}^{D_2O}K_5}{1 + C_{Vf} + C_r} \quad (A1)$$

$$C_{Vf} = k_5\left[\frac{k_8}{k_7k_9[O_2]} + \frac{1}{k_7} + \frac{1}{k_9} + \frac{1}{k_{11}} + \frac{1}{k_{13}} + \frac{1}{k_{15}}\right] \quad (A2)$$

$$C_r = k_6\left[\frac{1}{k_7[O_2]} + \frac{k_8}{k_7k_9[O_2]}\right] \quad (A3)$$

The parameters C_{Vf} and C_r are the forward and reverse commitments to catalysis, respectively. $^{D_2O}k_5$ is the kinetic SIE for water release; $^{D_2O}K_5$ is the equilibrium SIE on aquo release, and $^{D_2O}k_{15}$ is the kinetic SIE on water rebinding. The equations derived for the SIEs for $k_{cat}/K_{M(CTAD)}$, $k_{cat}/K_{M(\alpha KG)High[CTAD]}$, and $k_{cat}/K_{M(\alpha KG)Low[CTAD]}$ take a similar form and are shown below.

$$^{D_2O}\left[\frac{k_{cat}}{K_{M(\alpha KG)High[CTAD]}}\right] = \frac{^{D_2O}k_1\left(\frac{k_3[CTAD]}{k_2}\right) + {}^{D_2O}K_1}{1 + \frac{k_3[CTAD]}{k_2}} \quad (A4)$$

$$^{D_2O}\left[\frac{k_{cat}}{K_{M(\alpha KG)Low[CTAD]}}\right] = \left[{}^{D_2O}k_1\left(\frac{k_3[CTAD]k_5}{k_2k_4}\right) + {}^{D_2O}K_1\left(\frac{k_5}{k_4}\right) + {}^{D_2O}k_5{}^{D_2O}K_1 + C_r{}^{D_2O}K_1{}^{D_2O}K_5\right] \Big/ \left(1 + C_f + C_r\right) \quad (A5)$$

$$C_f = k_5\left(\frac{1}{k_4} + \frac{k_3[CTAD]}{k_2k_4}\right) \quad (A6)$$

$$C_r = k_6\left(\frac{1}{k_7[O_2]} + \frac{k_8}{k_7k_9[O_2]}\right) \quad (A7)$$

$$^{D_2O}\left[\frac{k_{cat}}{K_{M(CTAD)}}\right] = \frac{^{D_2O}k_5 + C_f + C_r{}^{D_2O}K_5}{1 + C_f + C_r} \quad (A8)$$

$$C_f = \frac{k_5}{k_4} \quad (A9)$$

$$C_r = k_6\left(\frac{1}{k_7[O_2]} + \frac{k_8}{k_7k_9[O_2]}\right) \quad (A10)$$

ASSOCIATED CONTENT

Supporting Information

Control experiments showing the effect of ionic strength and viscosity on the steady-state kinetics of FIH. This material is available free of charge via the Internet at http://pubs.acs.org.

AUTHOR INFORMATION

Corresponding Author

*Department of Chemistry, University of Massachusetts, Amherst, MA 01003. Phone: (413) 545-4001. Fax: (413) 545-4490. E-mail: mknapp@chem.umass.edu.

Funding

We thank the National Institutes of Health for Grant R01-GM077413.

Notes

The authors declare no competing financial interest.

ABBREVIATIONS

HIF, hypoxia inducible factor-1α; FIH, factor-inhibiting HIF; αKG, α-ketoglutarate; CTAD, C-terminal transactivation domain; CREB, cAMP response element-binding protein; CAS, clavaminate synthase; MCD, magnetic circular dichroism; CD, circular dichroism; HEPES, 4-(2-hydroxyethyl)-1-piperazineethanesulfonic acid; SIE, solvent isotope effect; ROS, reactive oxygen species; PHD2, prolyl hydroxylase dioxygenase 2; TauD, taurine dioxygenase; SLO, soybean lipoxygenase.

REFERENCES

(1) Hausinger, R. P. (2004) FeII/α-ketoglutarate-dependent hydroxylases and related enzymes. *Crit. Rev. Biochem. Mol. Biol. 39*, 21−68.

(2) Solomon, E. I., Brunold, T. C., Davis, M. I., Kemsley, J. N., Lee, S. K., Lehnert, N., Neese, F., Skulan, A. J., Yang, Y. S., and Zhou, J. (2000) Geometric and electronic structure/function correlations in non-heme iron enzymes. *Chem. Rev. 100*, 235−350.

(3) Costas, M., Mehn, M. P., Jensen, M. P., and Que, L., Jr. (2004) Dioxygen activation at mononuclear nonheme iron active sites: Enzymes, models, and intermediates. *Chem. Rev. 104*, 939−986.

(4) Hewitson, K. S., McNeill, L. A., Riordan, M. V., Tian, Y. M., Bullock, A. N., Welford, R. W., Elkins, J. M., Ooldham, N. J., Bhattacharya, S., Gleadle, J. M., Ratcliffe, P. J., Pugh, C. W., and Schofield, C. J. (2002) Hypoxia-inducible factor (HIF) asparagine hydroxylase is identical to factor inhibiting HIF (FIH) and is related to the cupin structural family. *J. Biol. Chem. 277*, 26351−26355.

(5) Ivan, M., Kondo, K., Yang, H., Kim, W., Valiando, J., Ohh, M., Salic, A., Asara, J. M., Lane, W. S., and Kaelin, W. G., Jr. (2001) HIFα targeted for VHL-mediated destruction by proline hydroxylation: Implications for O_2 sensing. *Science 292*, 464−468.

(6) Lando, D., Peet, D. J., Gorman, J. J., Whelan, D. a., Whitelaw, M. L., and Bruick, R. K. (2002) FIH-1 is an asparaginyl hydroxylase enzyme that regulates the transcriptional activity of hypoxia-inducible factor. *Genes Dev. 16*, 1466−1471.1.
(7) McNeill, L. A., Hewitson, K. S., Claridge, T. D., Seibel, J. F., Horsfall, L. E., and Schofield, C. J. (2002) Hypoxia-inducible factor asparaginyl hydroxylase (FIH-1) catalyses hydroxylation at the β-carbon of asparagine-803. *Biochem. J. 367*, 571−575.
(8) Zhou, J., Gunsior, M., Bachmann, B. O., Townsend, C. A., and Solomon, E. I. (1998) Substrate Binding to the α-Ketoglutarate-Dependent Non-Heme Iron Enzyme Clavaminate Synthase 2: Coupling Mechanism of Oxidative Decarboxylation and Hydroxylation. *J. Am. Chem. Soc. 120*, 13539−13540.
(9) Zhou, J., Kelly, W. L., Bachmann, B. O., Gunsior, M., Townsend, C. A., and Solomon, E. I. (2001) Spectroscopic studies of substrate interactions with clavaminate synthase 2, a multifunctional α-KG-dependent non-heme iron enzyme: Correlation with mechanisms and reactivities. *J. Am. Chem. Soc. 123*, 7388−7398.
(10) Pavel, E. G., Zhou, J., Busby, R. W., Gunsior, M., Townsend, C. A., and Solomon, E. I. (1998) Circular dichroism and magnetic circular dichroism spectroscopic studies of the non-heme ferrous active site in clavaminate synthase and its interaction with α-ketoglutarate cosubstrate. *J. Am. Chem. Soc. 120*, 743−753.
(11) Price, J. C., Barr, E. W., Hoffart, L. M., Krebs, C., and Bollinger, J. M. (2005) Kinetic dissection of the catalytic mechanism of taurine: α-Ketoglutarate dioxygenase (TauD) from *Escherichia coli*. *Biochemistry 44*, 8138−8147.
(12) Price, J. C., Barr, E. W., Tirupati, B., Bollinger, J. M., Jr., and Krebs, C. (2003) The first direct characterization of a high-valent iron intermediate in the reaction of an α-ketoglutarate-dependent dioxygenase: A high-spin FeIV complex in taurine/α-ketoglutarate dioxygenase (TauD) from *Escherichia coli*. *Biochemistry 42*, 7497−7508.
(13) Price, J. C., Barr, E. W., Glass, T. E., Krebs, C., and Bollinger, J. M., Jr. (2003) Evidence for hydrogen abstraction from C1 of taurine by the high-spin Fe(IV) intermediate detected during oxygen activation by taurine:α-ketoglutarate dioxygenase (TauD). *J. Am. Chem. Soc. 125*, 13008−13009.
(14) Saban, E., Chen, Y. H., Hangasky, J. A., Taabazuing, C. Y., Holmes, B. E., and Knapp, M. J. (2011) The Second Coordination Sphere of FIH Controls Hydroxylation. *Biochemistry 50*, 4733−4740.
(15) Elkins, J. M., Hewitson, K. S., McNeill, L. A., Seibel, J. F., Schlemminger, I., Pugh, C. W., Ratcliffe, P. J., and Schofield, C. J. (2003) Structure of factor-inhibiting hypoxia-inducible factor (HIF) reveals mechanism of oxidative modification of HIF-1α. *J. Biol. Chem. 278*, 1802−1806.
(16) Dann, C. E., Bruick, R. K., and Deisenhofer, J. (2002) Structure of factor-inhibiting hypoxia-inducible factor 1: An asparaginyl hydroxylase involved in the hypoxic response pathway. *Proc. Natl. Acad. Sci. U.S.A. 99*, 15351−15356.
(17) Chen, Y.-H., Comeaux, L. M., Eyles, S. J., and Knapp, M. J. (2008) Auto-hydroxylation of FIH-1, an Fe(II), α-ketoglutarate dependent human hypoxia sensor. *Chem. Commun.*, 4768−4770.
(18) Chen, Y. H., Comeaux, L. M., Herbst, R. W., Saban, E., Kennedy, D. C., Maroney, M. J., and Knapp, M. J. (2008) Coordination changes and auto-hydroxylation of FIH-1: Uncoupled O_2-activation in a human hypoxia sensor. *J. Inorg. Biochem. 102*, 2120−2129.
(19) Yang, M., Chowdhury, R., Ge, W., Hamed, R. B., McDonough, M. A., Claridge, T. D. W., Kessler, B. M., Cockman, M. E., Ratcliffe, P. J., and Schofield, C. J. (2011) Factor-inhibiting hypoxia-inducible factor (FIH) catalyses the post-translational hydroxylation of histidinyl residues within ankyrin repeat domains. *FEBS J. 278*, 1086−1097.
(20) Coleman, M. L., McDonough, M. A., Hewitson, K. S., Coles, C., Mecinovic, J., Edelmann, M., Cook, K. M., Cockman, M. E., Lancaster, D. E., Kessler, B. M., Oldham, N. J., Ratcliffe, P. J., and Schofield, C. J. (2007) Asparaginyl hydroxylation of the notch ankyrin repeat domain by factor inhibiting hypoxia-inducible factor. *J. Biol. Chem. 282*, 24027−24038.
(21) Saban, E., Flagg, S. C., and Knapp, M. J. (2011) Uncoupled O_2-activation in the human HIF-asparaginyl hydroxylase, FIH, does not produce reactive oxygen species. *J. Inorg. Biochem. 105*, 630−636.
(22) *CRC Handbook of Chemistry and Physics*, 61st ed. (1981) CRC Press, Boca Raton, FL.
(23) Quinn, D. M., and Sutton, L. D. (1991) Theoretical Basis and Mechanistic Utility of Solvent Isotope Effects. In *Enzyme Mechanism from Isotope Effects* (Cook, P. F., Ed.) pp 73−126, CRC Press, Boca Raton, FL.
(24) Flashman, E., Hoffart, L. M., Hamed, R. B., Bollinger, J. M., Krebs, C., and Schofield, C. J. (2010) Evidence for the slow reaction of hypoxia-inducible factor prolyl hydroxylase 2 with oxygen. *FEBS J. 277*, 4089−4099.
(25) *Enzyme Mechanism from Isotope Effects* (1991) CRC Press, Boca Raton, FL.
(26) McFarland, J., and Bernhard, S. A. (1972) Catalytic Steps During Single-Turnover Reduction of Aldehydes by Alcohol-Dehydrogenase. *Biochemistry 11*, 1486.
(27) Lee, K. M., Dahlhauser, K. F., and Plapp, B. V. (1988) Reactivity of Horse Liver Alcohol-Dehydrogenase with 3-Methylcyclohexanols. *Biochemistry 27*, 3528−3532.
(28) Dunn, M. F., and Hutchison, J. S. (1973) Roles of zinc ion and reduced coenzyme in the formation of a transient chemical intermediate during the equine liver alcohol dehydrogenase catalyzed reduction of an aromatic aldehyde. *Biochemistry 12*, 4882−4892.
(29) Kassebaum, J. W., and Silverman, D. N. (1989) Hydrogen/deuterium fractionation factors of the aqueous ligand of cobalt in $Co(H_2O)_{62}^{+}$ and Co(II)-substituted carbonic anhydrase. *J. Am. Chem. Soc. 111*, 2691−2696.
(30) Cook, P. F. (1991) Kinetic and regulatory mechanisms of enzymes from isotope effects. In *Enzyme Mechanism from Isotope Effects*, pp 203−230, CRC Press, Boca Raton, FL.
(31) Koivunen, P., Hirsilä, M., Günzler, V., Kivirikko, K. I., and Myllyharju, J. (2004) Catalytic properties of the asparaginyl hydroxylase (FIH) in the oxygen sensing pathway are distinct from those of its prolyl 4-hydroxylases. *J. Biol. Chem. 279*, 9899−9904.
(32) Blacklow, S. C., Raines, R. T., Lim, W. a., Zamore, P. D., and Knowles, J. R. (1988) Triosephosphate isomerase catalysis is diffusion controlled. *Biochemistry 27*, 1158−1167.
(33) Brouwer, A. C., and Kirsch, J. F. (1982) Investigation of diffusion-limited rates of chymotrypsin reactions by viscosity variation. *Biochemistry 21*, 1302−1307.
(34) Raber, M. L., Freeman, M. F., and Townsend, C. A. (2009) Dissection of the Stepwise Mechanism to β-Lactam Formation and Elucidation of a Rate-determining Conformational Change in β-Lactam Synthetase. *J. Biol. Chem. 284*, 207−217.
(35) Karsten, W. E., Lai, C.-J., and Cook, P. F. (1995) Inverse Solvent Isotope Effects in the NAD-Malic Enzyme Reaction Are the Result of the Viscosity Difference between D_2O and H_2O: Implications for Solvent Isotope Effect Studies. *J. Am. Chem. Soc. 117*, 5914−5918.
(36) Holme, E. (1975) Kinetic study of thymine 7-hydroxylase from *Neurospora crassa*. *Biochemistry 14*, 4999−5003.
(37) Rundgren, M. (1977) Steady state kinetics of 4-hydroxyphenylpyruvate dioxygenase from human liver (III). *J. Biol. Chem. 252*, 5094−5099.
(38) De Carolis, E., and De Luca, V. (1993) Purification, characterization, and kinetic analysis of a 2-oxoglutarate-dependent dioxygenase involved in vindoline biosynthesis from *Catharanthus roseus*. *J. Biol. Chem. 268*, 5504−5511.
(39) Cook, P. F., and Cleland, W. W. (2007) *Enzyme Kinetics and Mechanism*, Garland Science, New York.
(40) Izquierdo, M. C., and Stein, R. L. (1990) Mechanistic studies of thermolysin. *J. Am. Chem. Soc. 112*, 6054−6062.
(41) Born, T. L., Zheng, R., and Blanchard, J. S. (1998) Hydrolysis of N-succinyl-L,L-diaminopimelic acid by the *Haemophilus influenzae* dapE-encoded desuccinylase: Metal activation, solvent isotope effects, and kinetic mechanism. *Biochemistry 37*, 10478−10487.

(42) Harrison, R. K., Chang, B., Niedzwiecki, L., and Stein, R. L. (1992) Mechanistic studies on the human matrix metalloproteinase stromelysin. *Biochemistry 31*, 10757−10762.
(43) Tomchick, D. R., Phan, P., Cymborowski, M., Minor, W., and Holman, T. R. (2001) Structural and Functional Characterization of Second-Coordination Sphere Mutants of Soybean Lipoxygenase-1. *Biochemistry 40*, 7509−7517.
(44) Cook, P. F., and Cleland, W. W. (1981) Mechanistic deductions from isotope effects in multireactant enzyme mechanisms. *Biochemistry 20*, 1790−1796.
(45) Northrop, D. B. (1977) *Isotope Effects on Enzyme-Catalyzed Reactions*, University Park Press, Baltimore.
(46) Grzyska, P. K., Ryle, M. J., Monterosso, G. R., Liu, J., Ballou, D. P., and Hausinger, R. P. (2005) Steady-State and Transient Kinetic Analyses of Taurine/α-Ketoglutarate Dioxygenase: Effects of Oxygen Concentration, Alternative Sulfonates, and Active-Site Variants on the FeIV-oxo Intermediate. *Biochemistry 44*, 3845−3855.
(47) Flagg, S. C., Giri, N., Pektas, S., Maroney, M. J., and Knapp, M. J. (2012) Inverse Solvent Isotope Effects Demonstrate Slow Aquo Release from Hypoxia Inducible Factor-Prolyl Hydroxylase (PHD2). *Biochemistry 51*, 6654−6666.
(48) Neidig, M. L., Brown, C. D., Light, K. M., Fujimori, D. G., Nolan, E. M., Price, J. C., Barr, E. W., Bollinger, J. M., Krebs, C., Walsh, C. T., and Solomon, E. I. (2007) CD and MCD of CytC3 and taurine dioxygenase: Role of the facial triad in α-KG-dependent oxygenases. *J. Am. Chem. Soc. 129*, 14224−14231.
(49) Ryle, M. J., Liu, A., Muthukumaran, R. B., Ho, R. Y. N., Koehntop, K. D., McCracken, J., Que, L., and Hausinger, R. P. (2003) O_2- and α-Ketoglutarate-Dependent Tyrosyl Radical Formation in TauD, an α-Keto Acid-Dependent Non-Heme Iron Dioxygenase. *Biochemistry 42*, 1854−1862.
(50) Koehntop, K. D., Marimanikkuppam, S., Ryle, M. J., and Hausinger, R. P. (2006) Self-hydroxylation of taurine/α-ketoglutarate dioxygenase: Evidence for more than one oxygen activation mechanism. *J. Biol. Inorg. Chem.*, 63−72.
(51) Tian, G. C. (1992) Effective Rate Constants and General Isotope Effect Equations for Steady-State Enzymatic-Reactions with Multiple Isotope-Sensitive Steps. *Bioorg. Chem. 20*, 95−106.